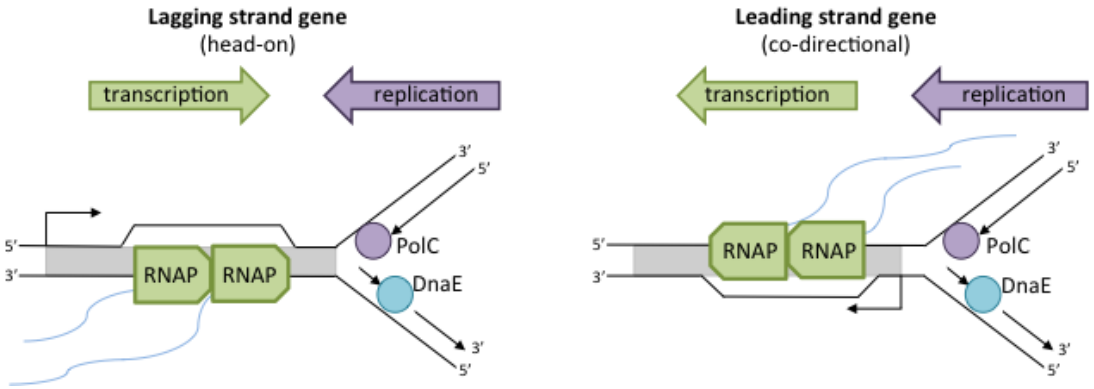

Figure S1. RNA and DNA Polymerases proceed in a 3' to 5' direction on the template strand while synthesizing 5' to 3'. For a lagging strand-encoded gene, the two machineries move in opposite directions, and the template strand is replicated discontinuously. Leading strand encoded genes are transcribed in the same direction as the continuously replicated template strand.

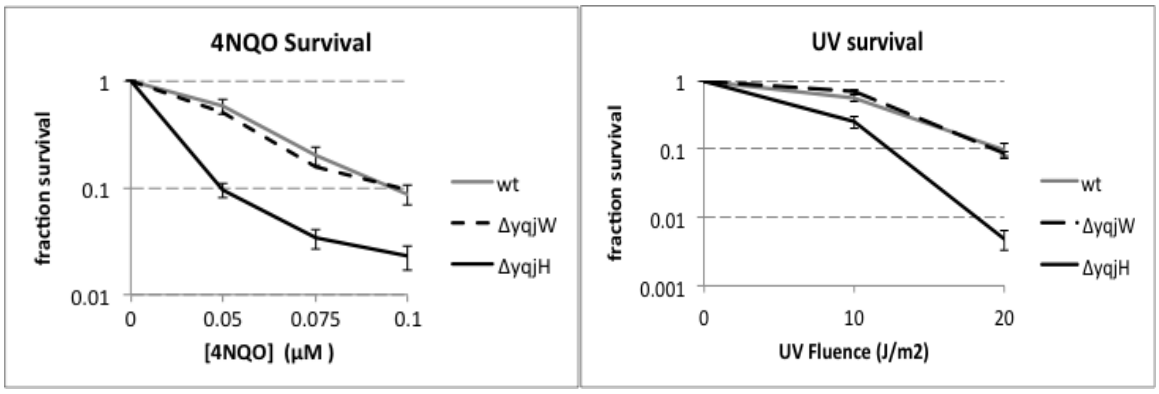

Figure S2. Survival assays were performed in wild type (HM1, gray lines), Δ*yqjH* (HM391, black lines), and Δ*yqjW* (HM425, dashed lines) strains as described in **supplementary methods**. Data shown is the average from 8 (UV) or 12 (4NQO) biological replicates, error bars represent standard deviations.

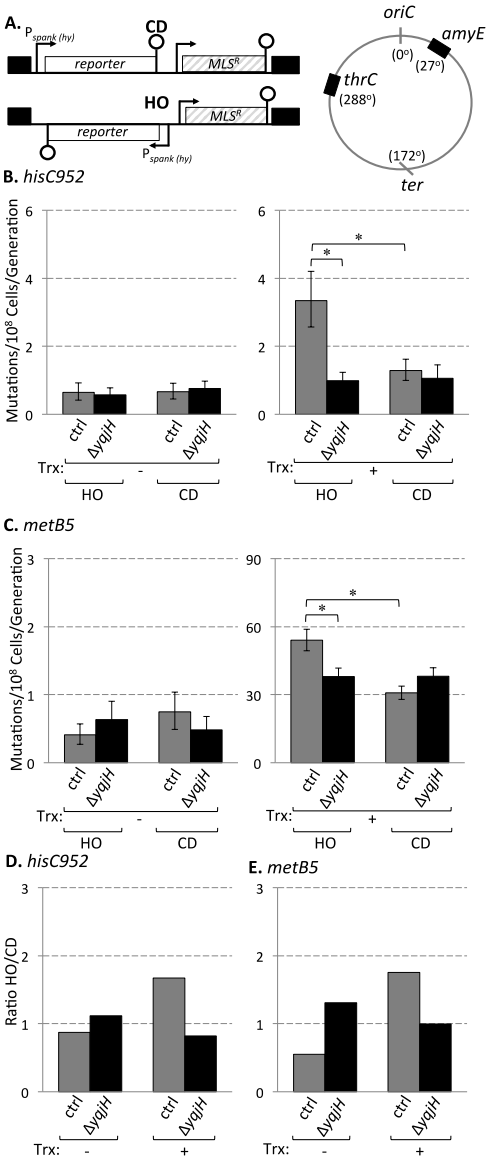

Figure S3. A. Schematic of the *thrC* locus harboring mutation reporters oriented head-on (HM449 and HM672) or co-directionally (HM450 and HM673) to replication, as well as a chromosomal map depicting the positions of both the *amyE* and *thrC* loci. **B.** Mutation rates were estimated for the *hisC952* reporter (CAG➔TAG) at the *thrC* locus in the presence (HM449 and HM450; gray bars), or absence of *yqjH* (HM611 and HM612; black bars), for the head-on and co-directional orientations, with (Trx+) and without (Trx-) IPTG. **C.** Same as **B.** for the *metB5* (GAA➔TAA) reporter at the t*hrC* locus (HM449 and HM450, ctrl, gray bars; HM674 and HM675, Δ*yajH,* black bars. **D.** The ratio of mutation rates in the presence of transcription for the head-on to co-directional orientation is plotted for strains harboring the *hisC952*, in both wild-type (gray bars) and *ΔyqjH* mutant backgrounds (black bars). **E.** Same as **D.** for the *metB5* reporters. Mutation rates were estimated based on C=36-48, for each strain and condition. Error bars are 95% confidence intervals, (*P<0.05).

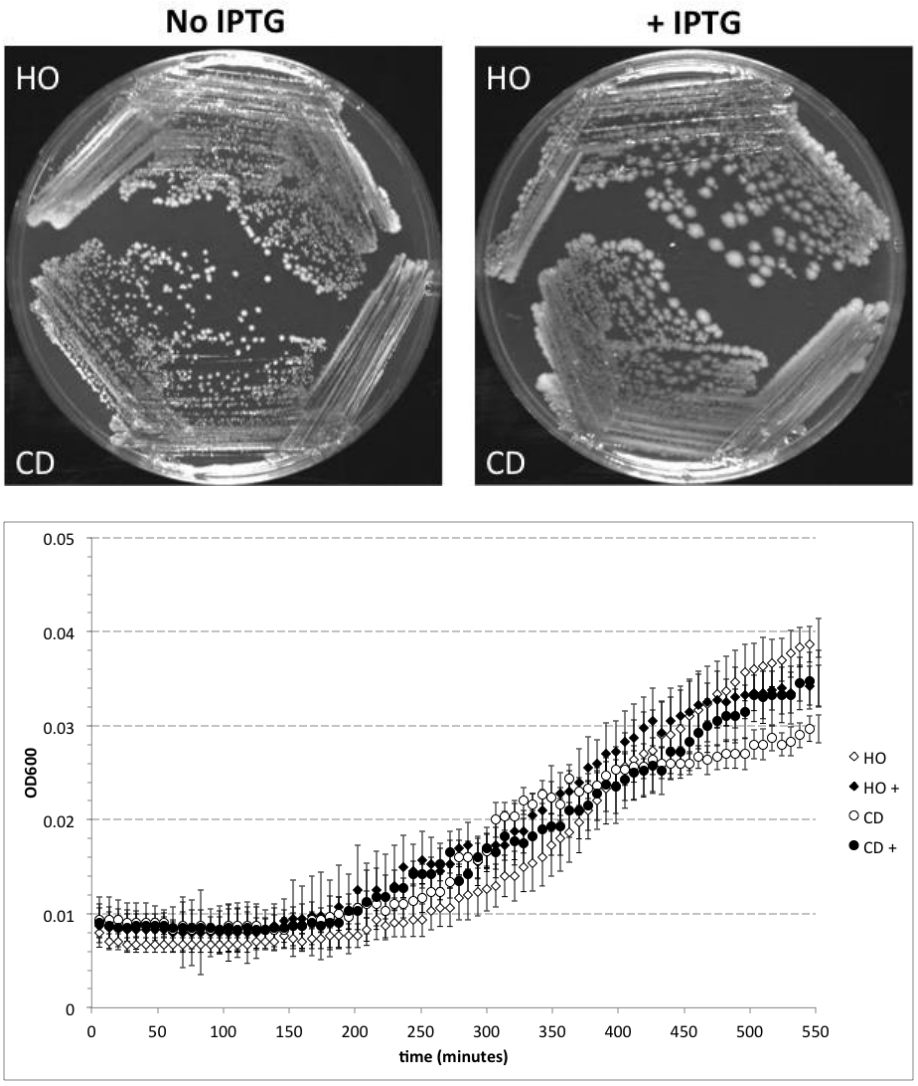

Figure S4. Strains 1177 (HO) and 1178 (CD), which harbor wild type alleles of *hisC* under control of $P_{spank\ (hy)}$ were streaked from freezer stocks onto plates containing minimal medium lacking histidine with or without IPTG. Additionally, growth curves were obtained in minimal medium lacking histidine for each strain with (+) or without IPTG.

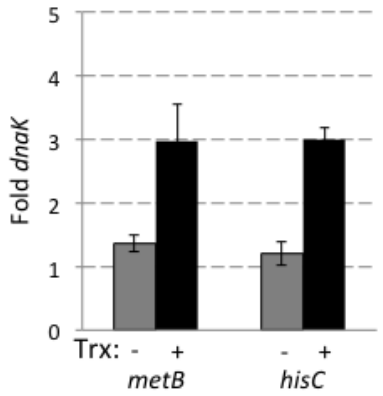

Figure S5. RNA levels for the *metB5* (HM633) and *hisC952* (HM420) reporter strains, normalized to *dnaK*, for the CD orientation, with (Trx+, gray bars) and without (Trx-, black bars) IPTG. Data shown is the average from 6 biological replicates; error bars represent standard error of the mean.

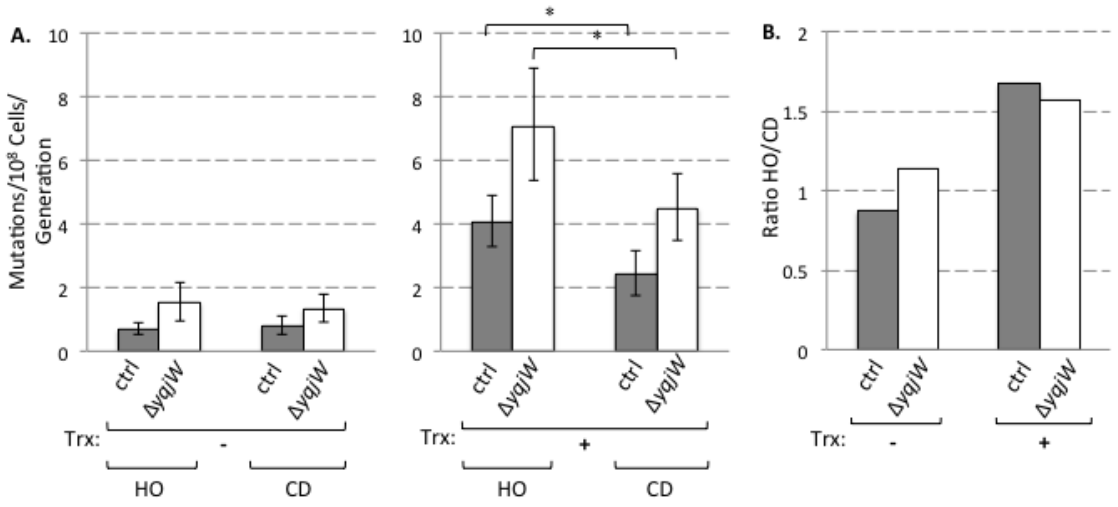

Figure S6. A. Mutation rates for the *hisC952* reporter in the presence (HM419 and HM420; gray bars), or absence of PolY2 (*ΔyqjW*) (HM425 and HM426; black bars), for the head-on and co-directional orientations, with (Trx+) and without (Trx-) IPTG. **B.** The ratio of mutation rates for the head-on to co-directional orientations for strains HM419/HM420 ("ctrl,"gray bars) as well as for strains HM425/HM426 ("Δ*yqjW*," white bars) in the presence (Trx +) and absence (Trx -) of 1mM IPTG. Mutation rates were estimated based on C=36-48, for each strain and condition. Error bars are 95% confidence intervals, (*P<0.05).

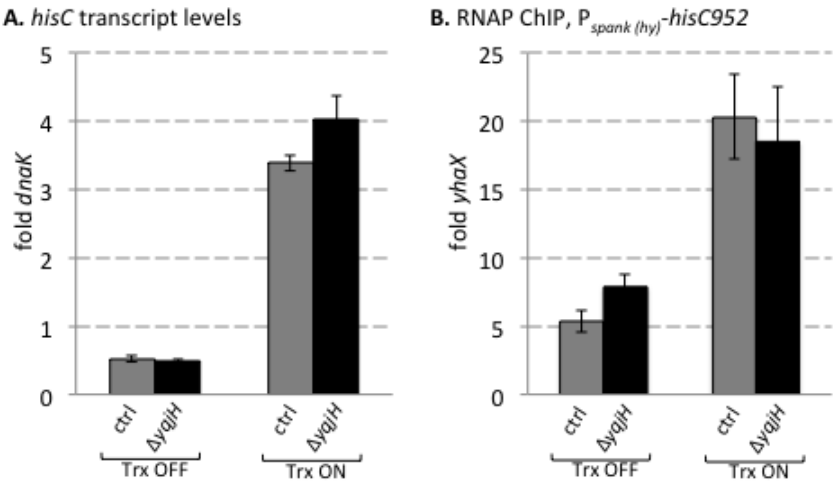

Figure S7. A. RNA levels for the *hisC952* reporter strains, normalized to *dnaK,* (HM419, ctrl, gray bars; HM421 and HM4222, Δ*yajH,* black bars) with (Trx+) and without (Trx-) IPTG. **B**. Relative association of RpoC by ChIP–qPCR with the region harboring $P_{spank(hy)}$-*hisC952* reporter gene, compared to the control region *yha*X (HM419, ctrl, gray bars; HM421 and HM4222, Δ*yajH,* black bars), with (Trx+) and without (Trx-) IPTG. Error bars represent standard error. Data is from 3 independent experiments (n=9).

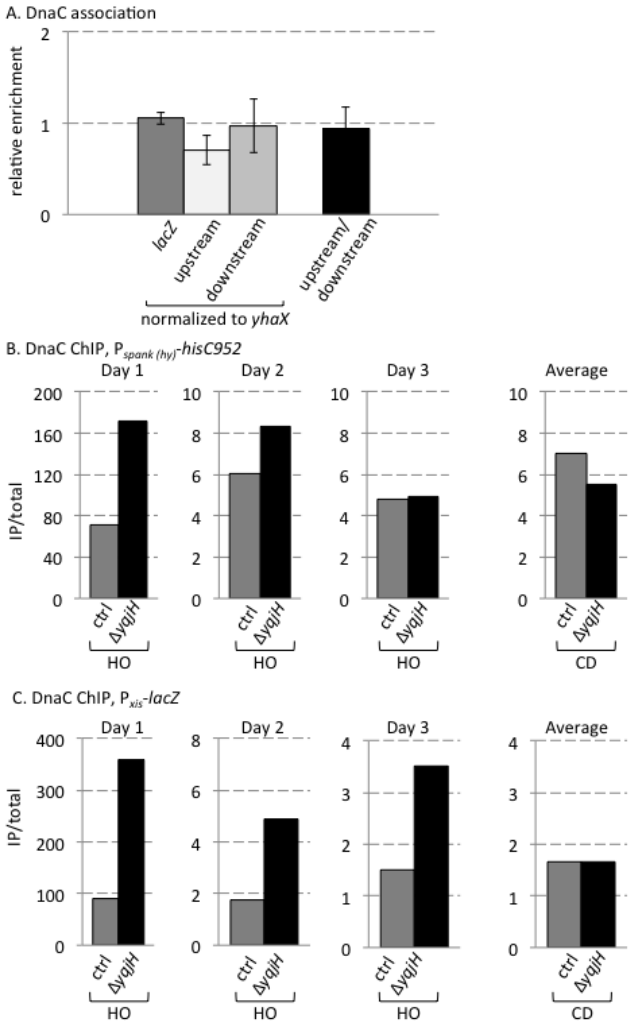

Figure S8. A. Relative association of DnaC with regions 1 kb upstream (*guaC* locus) and 1 kb downstream (intragenic region) of *thrC* in strains harboring the P_{xis}-*lacZ* reporter gene, compared to the control region *yha*X was analyzed by ChIP–qPCR in the absence of transcription. Data shown represents averages of nine biological replicates. **B.** Absolute ChIP signal for the enrichment of DnaC at the *hisC952* conflict region relative to total input samples for three independent experiments for the head on orientation, and the average of three experiments for the co-directional orientation is shown. **C.** Absolute ChIP signal for the enrichment of DnaC at the *lacZ* conflict region relative to total input samples for three independent experiments for the head on orientation, and the average of three experiments for the co-directional orientation is shown. Error bars represent standard error. (n=12) (** P<0.01, ***P<0.005).

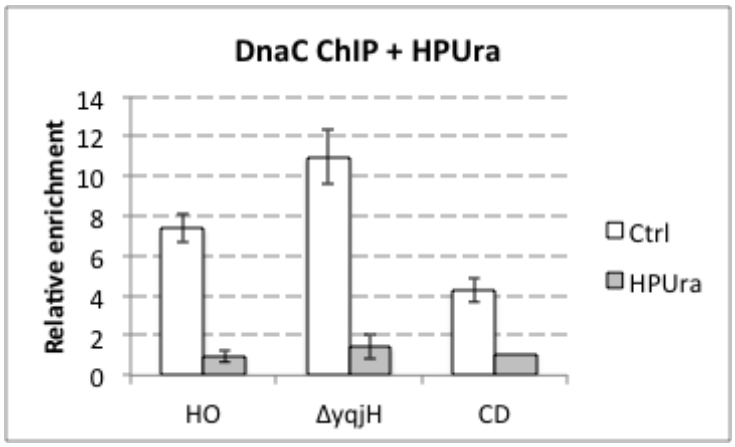

Figure S9. Relative association of DnaC in strains expressing the P_{xis}-*lacZ* reporter gene, compared to the control region *yha*X was analyzed by ChIP–qPCR in the presence (HPUra, gray bars) and absence (ctrl, white bars) of the replication inhibitor HPUra at a concentration of 38.6 µg/ml. Data shown is the average of 3-9 biological replicates. Error bars represent standard deviations.

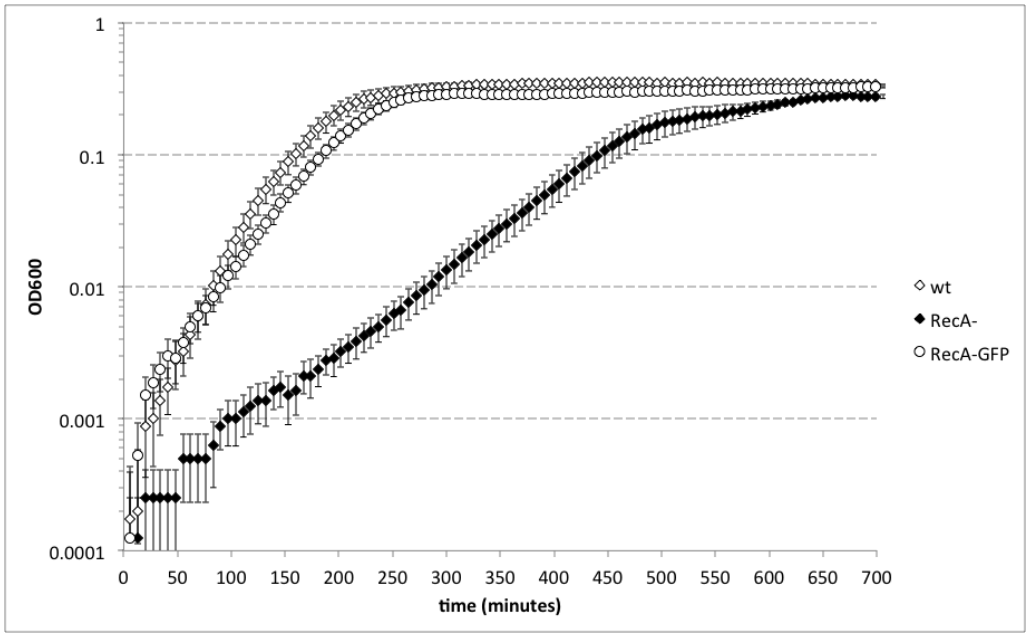

Figure S10. Growth curves in LB medium were obtained for strains expressing the P_{xis}-*lacZ* reporter in wt backgrounds (HM211, wt, white diamonds), backgrounds with *recA* deleted (HM824, RecA-, black diamonds), or backgrounds harboring RecA-GFP (HM352, RecA-GFP). Data shown is the average of eight biological replicates grown on two different days.

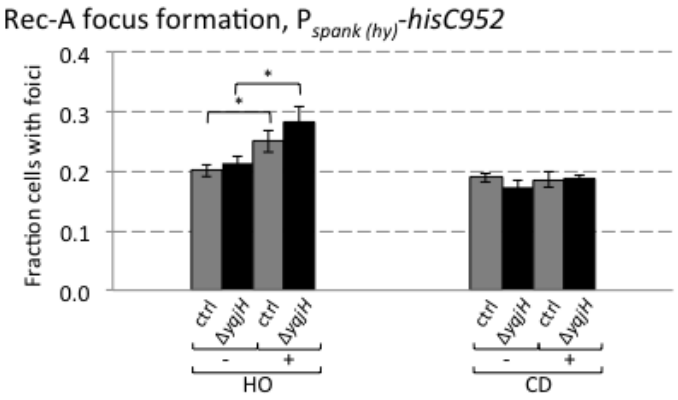

Figure S11. A. Microscopy was performed and RecA-GFP focus formation quantified as described in **methods** for strains harboring the *hisC952* reporter in the presence (HM594 and HM595; gray bars), or absence of *yqjH* (HM596 and HM597; black bars), for the head-on and co-directional orientations, with (Trx+) and without (Trx-) IPTG. The increased RecA-GFP focus formation between the transcription off and transcription on condition is statistically significant (P=0.01).

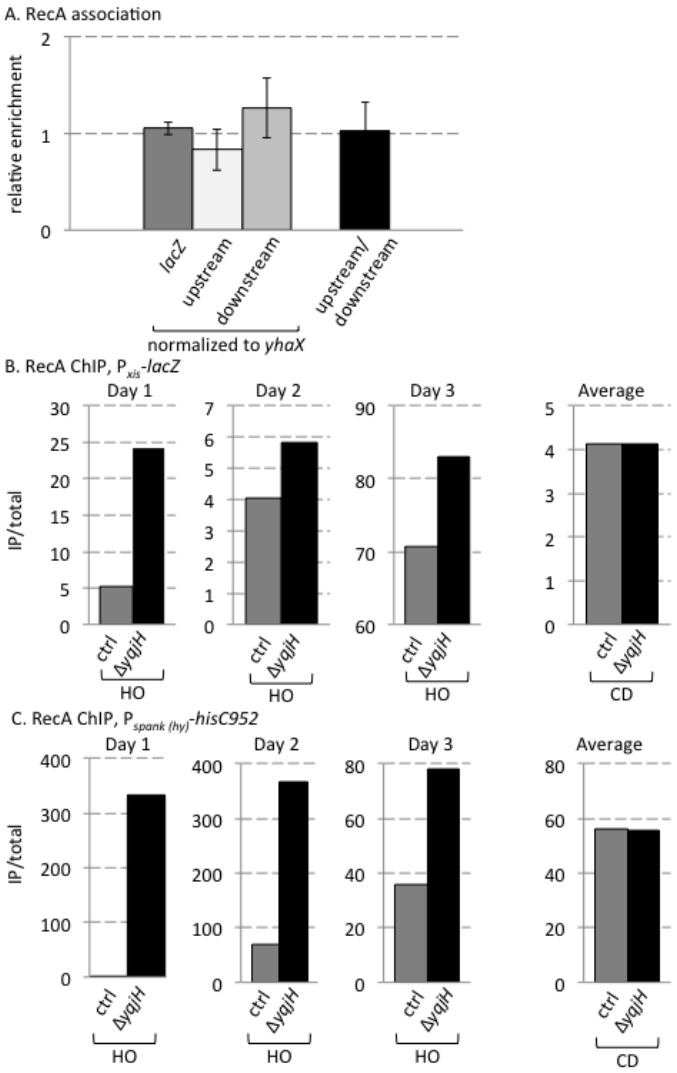

Figure S12. A. Relative association of RecA with regions 1 kb upstream (*guaC* locus) and 1 kb downstream (intragenic region) of *thrC* in strains harboring the P_{xis}-*lacZ* reporter gene, compared to the control region *yh*aX was analyzed by ChIP–qPCR in the absence of transcription. Data shown represents averages of nine biological replicates. **B.** Absolute ChIP signal for the enrichment of RecA at the *lacZ* conflict region relative to total input samples for three independent experiments for the head on orientation, and the average of three experiments for the co-directional orientation is shown. **C.** Absolute ChIP signal for the enrichment of RecA at the *hisC* conflict region relative to total input samples for three independent experiments for the head on orientation, and the average of three experiments for the co-directional orientation is shown. Error bars represent standard error. (n=6-12) (**P<0.01, ***P<0.005, ****P<0.001).

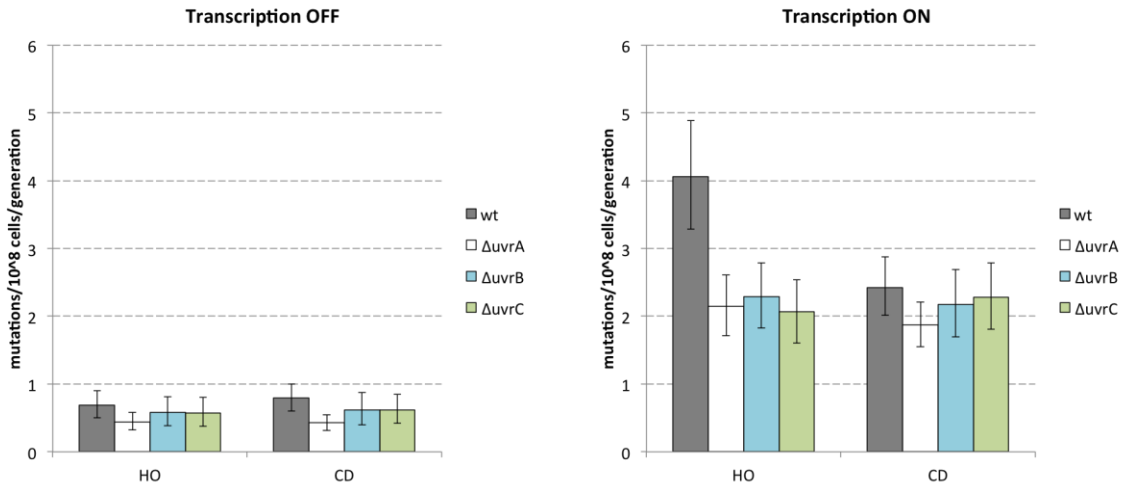

Figure S13. A. Mutation rates for the *hisC952* reporter in the presence (HM419 and HM420; gray bars), or absence of UvrA (*ΔuvrA*) (HM735 and HM736; white bars), UvrB (*ΔuvrB*) (HM1281 and HM1282; teal bars), or UvrC (*ΔuvrC*) (HM1283 and HM1284; teal bars), for the head-on and co-directional orientations, with (Transcription ON, right panel) and without (Transcription OFF, left panel) IPTG. Mutation rates were estimated based on C=30-36, for each strain and condition. Error bars are 95% confidence intervals.

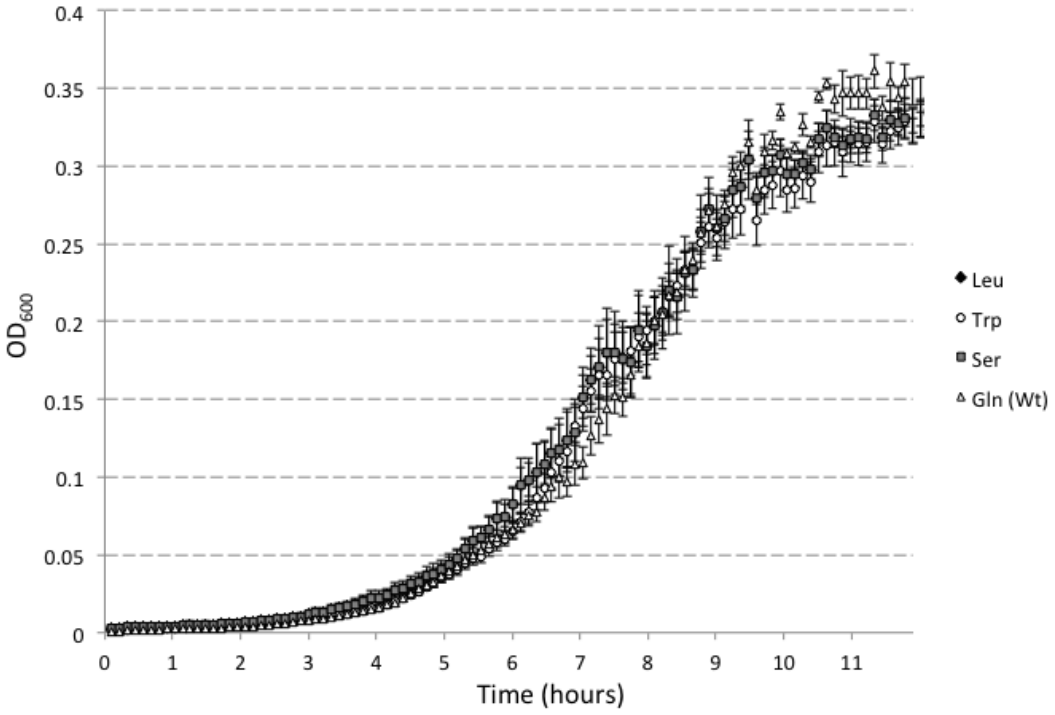

Figure S14. Growth curves were obtained in minimal medium lacking histidine for strains harboring the *hisC* mutation reporter with different base pair mutations, and thus differing amino acids, at the position of the stop codon. Data shown is average optical density measurements taken over time for four independent clones of each *hisC* allele.

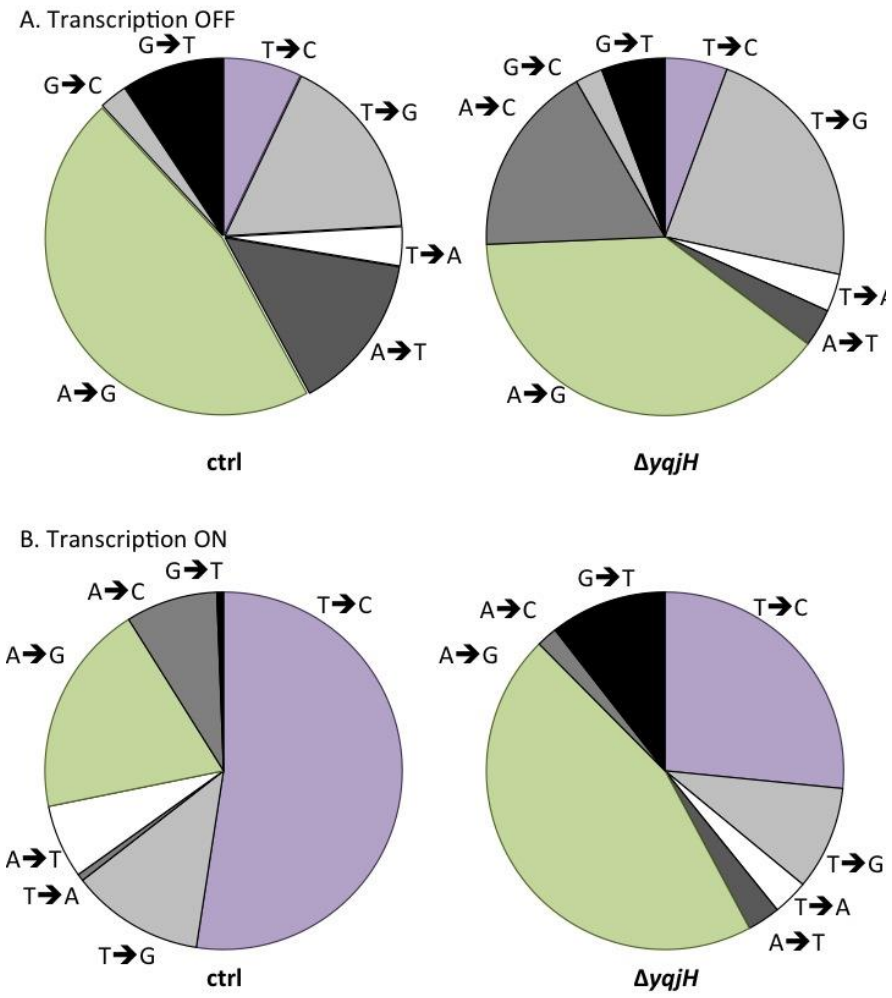

Figure S15. Frequencies for each observed point mutation leading to reversion of the *hisC952* reporter in the head-on orientation for wt cells (left chart) and cells lacking PolY1 (*ΔyqjH,* right chart) grown in **A.** the absence (transcription OFF) or **B.** in the presence of IPTG (transcription ON). Mutation frequency is calculated as the ratio of reads for a particular mutation divided by the total number of reads.

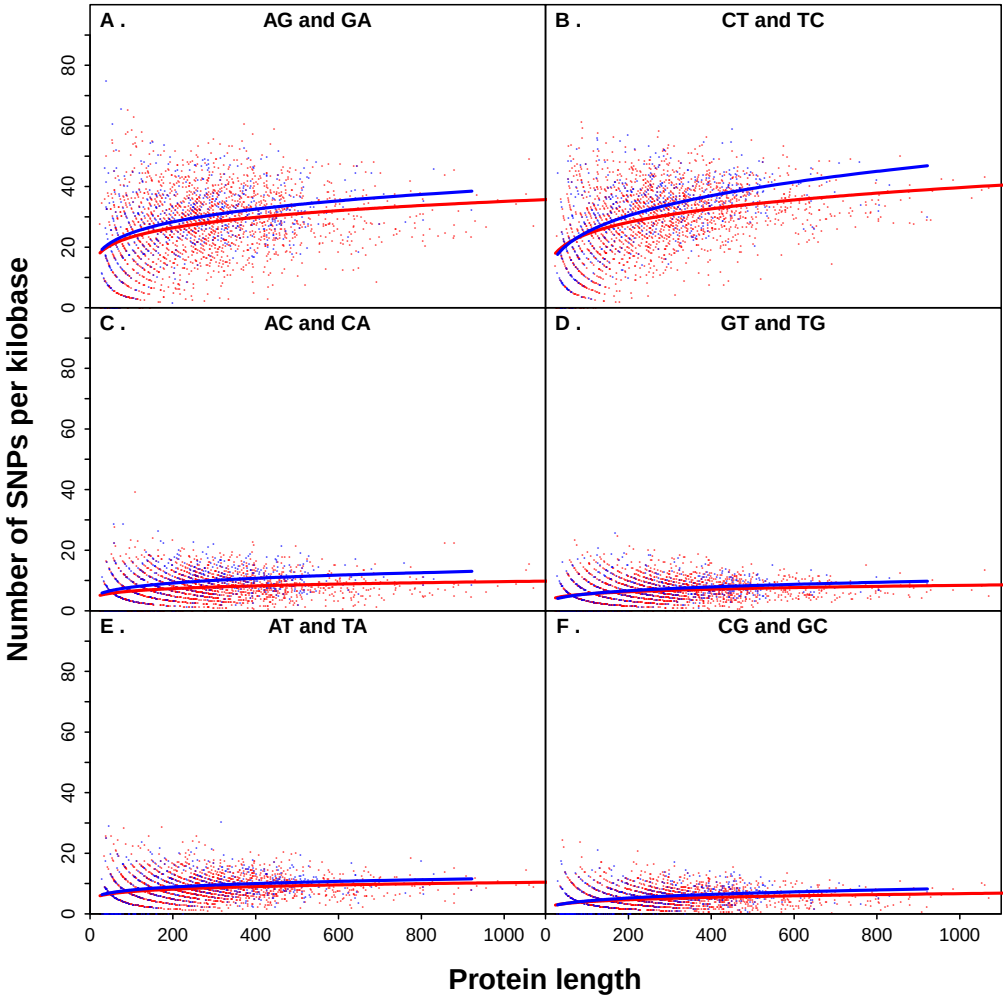

Figure S16. Only the TC/CT transitions show a significantly greater rate of mutation on the lagging versus the leading strand. The mutation rate (SNPs per kilobase) for each gene on the lagging strand (blue dots) and the leading strand (red dots) is shown as a function of its (translated) protein length. A large dispersion in mutation rates is evidence of the large range of gene conservation represented on both strands. The modeled mutation rates for the lagging strand (blue lines) and the leading strand (red lines) show the non-linear increase in the rates with gene length. The rates are higher for the GA/AG and TC/CT mutations. The difference in the rate of increase on the lagging strand compared to the leading strand of 4.5%/kb is significantly greater (p=0.005) for the TC/CT mutation (see Table S1).

Mutation	%/kb increase (lagging)	%/kb increase (leading)	p-value
CA/AC	16.7	14.8	NS
GA/AG	14.9	14.9	NS
TA/AT	9.5	10.8	NS
GC/CG	24.7	19.7	NS
TC/CT	25.3	20.8	0.07
TG/GT	19.3	14.8	NS

Table S1. The modeled mutation rate increases non-linearly with gene length on the lagging and leading strands. The percent increase in the mutation rate per kilobase of gene length is shown for the leading and lagging strands for pooled mutations (since direction of mutation is unknown). This non-linear increase in the mutation rate, modeled using negative binomial regression, had statistical significance ($p<0.0001$) for all mutations on the lagging strand (not shown). For all mutations, the increase in mutation rate with gene length is greater on the lagging strand than the leading strand. For most mutation pairs, the statistical support for the difference in the increase between the leading and lagging strand (p-value) is not significant (NS). Only the pooled TC + CT mutations achieved statistical significance ($p=0.005$) in the difference in rate between the strands.

Table S2. Strains used and generated in this study

Strain	Genotype	Reference
HM1	*trpC2, pheA1*	
HM209	*trpC2, pheA1, ΔrecA-MLS/CAT*	
HM210	*trpC2, pheA1, thrC*::P_{xis}-*lacZ,*	Merrikh, *Nature*, 2011
HM211	*trpC2, pheA1, thrC*::P_{xis}-*lacZ* ICE*Bs1*(0)	Merrikh, *Nature*, 2011
HM253	*trpC2, pheA1*, ICE*Bs1*(0)	Merrikh, *Nature*, 2011
HM313	*trpC2, pheA1, recA-mGFP*mut2-*spec*^{R}	Simmons, *PNAS*, 2007
HM352	*trpC2, pheA1, thrC*::P_{xis}-*lacZ*, ICE*Bs1*(0), *recA-mGFP*mut2-*spec*^{R}	Merrikh, *Nature*, 2011
HM391	*trpC2, pheA1, yqjH::CAT*	This study
HM380 (YB955)	*hisC952, metB5, leuC427,* SPβ^{sens}, xin^{-1}	Yasbin, *Genetics of industrial microorganisms*, 1987
HM415	*trpC2, pheA1, addAB::KAN*	This study
HM417	*hisC952, metB5, leuC427,* SPβ^{sens}, xin^{-1}, *amyE::*$P_{spank\ (hy)}$-*leuC4272* [head-on] *spec*^{R}	This study
HM418	*hisC952, metB5, leuC427,* SPβ^{sens}, xin^{-1}, *amyE::*$P_{spank\ (hy)}$-*leuC427* [co-directional] *spec*^{R}	This study
HM419	*hisC952, metB5, leuC427,* SPβ^{sens}, xin^{-1}, *amyE::*$P_{spank\ (hy)}$-*hisC952* [head-on] *spec*^{R}	Paul, *Nature*, 2013
HM420	*hisC952, metB5, leuC427,* SPβ^{sens}, xin^{-1}, *amyE::*$P_{spank\ (hy)}$-*hisC952* [co-directional] *spec*^{R}	Paul, *Nature*, 2013
HM421	*hisC952, metB5, leuC427,* SPβ^{sens}, xin^{-1}, *amyE::*$P_{spank\ (hy)}$-*hisC952* [head-on] *spec*^{R}, *yqjH::CAT*	This study
HM422	*hisC952, metB5, leuC427,* SPβ^{sens}, xin^{-1}, *amyE::*$P_{spank\ (hy)}$-*hisC952* [co-directional] *spec*^{R}, *yqjH::CAT*	This study
HM425	*hisC952, metB5, leuC427,* SPβ^{sens}, xin^{-1}, *amyE::*$P_{spank\ (hy)}$-*hisC952* [head-on] *spec*^{R}, *yqjW::CAT*	This study

HM426	*hisC952, metB5, leuC427,* SPβ^{sens}, xin^{-1}, *amyE::P$_{spank\ (hy)}$-hisC952* [co-directional] *spec^{R}, yqjW::CAT*	This study
HM445	*hisC952, metB5, leuC427,* SPβ^{sens}, xin^{-1}, *amyE::P$_{spank\ (hy)}$-hisC952* [head-on] *spec^{R}, mfd::*Cm^{R}	This study
HM444	*hisC952, metB5, leuC427,* SPβ^{sens}, xin^{-1}, *amyE::P$_{spank\ (hy)}$- hisC952* [co-directional] *spec^{R}, mfd::*Cm^{R}	This study
HM449	*hisC952, metB5, leuC427,* SPβ^{sens}, xin^{-1}, *thrC::P$_{spank\ (hy)}$-hisC952* [head-on] *MLS^{R}*	This study
HM450	*hisC952, metB5, leuC427,* SPβ^{sens}, xin^{-1}, *thrC::P$_{spank\ (hy)}$-hisC952* [co-directional] *MLS^{R}*	This study
HM594	*hisC952, metB5, leuC427,* SPβ^{sens}, xin^{-1}, *thrC::P$_{spank\ (hy)}$-hisC952* [head-on] *MLS^{R}, recA-GFP-spec^{R}*	This study
HM595	*hisC952, metB5, leuC427,* SPβ^{sens}, xin^{-1}, *thrC::P$_{spank\ (hy)}$-hisC952* [co-directional] *MLS^{R} recA-GFP-spec^{R}*	This study
HM596	*hisC952, metB5, leuC427,* SPβ^{sens}, xin^{-1}, *thrC::P$_{spank\ (hy)}$-hisC952* [head-on] *MLS^{R}, yqjH::CAT recA-GFP-spec^{R}*	This study
HM597	*hisC952, metB5, leuC427,* SPβ^{sens}, xin^{-1}, *thrC::P$_{spank\ (hy)}$-hisC952* [co-directional] *MLS^{R}, yqjH::CAT recA-GFP-spec^{R}*	This study
HM611	*hisC952, metB5, leuC427,* SPβ^{sens}, xin^{-1}, *thrC::P$_{spank\ (hy)}$-hisC952* [head-on] *MLS^{R}, yqjH::CAT*	This study
HM612	*hisC952, metB5, leuC427,* SPβ^{sens}, xin^{-1}, *thrC::P$_{spank\ (hy)}$-hisC952* [co-directional] *MLS^{R}, yqjH::CAT*	This study
HM629	*trpC2, pheA1, thrC*::*P$_{xis}$-lacZ* [head-on] *MLS^{R} yqjH::CAT* ICE*Bs*1(0)	This study
HM630	*trpC2, pheA1, thrC*::*P$_{xis}$-lacZ* [head-on] *MLS^{R}, recA-mGFP*mut2-*spec^{R}*	This study

HM631	*trpC2, pheA1, thrC*::P_{xis}-*lacZ* [head-on] MLS^R, *yqjH::CAT, recA-mGFP*mut2-$spec^R$	This study
HM632	*hisC952, metB5, leuC427,* $SP\beta^{sens}$, xin^{-1}, *amyE::*$P_{spank\ (hy)}$-*metB5* [head-on] $spec^R$	This study
HM633	*hisC952, metB5, leuC427,* $SP\beta^{sens}$, xin^{-1}, *amyE::*$P_{spank\ (hy)}$-*metB5* [co-directional] $spec^R$	This study
HM634	*hisC952, metB5, leuC427,* $SP\beta^{sens}$, xin^{-1}, *amyE::*$P_{spank\ (hy)}$-*metB5* [head-on] $spec^R$, *yqjH::CAT*	This study
HM635	*hisC952, metB5, leuC427,* $SP\beta^{sens}$, xin^{-1}, *amyE::*$P_{spank\ (hy)}$-*metB5* [co-directional] $spec^R$, *yqjH::CAT*	This study
HM639	*trpC2, pheA1, thrC*::P_{xis}-*lacZ* [co-directional] MLS^R	This study
HM640	*trpC2, pheA1, thrC*::P_{xis}-*lacZ* [co-directional] MLS^R, ICE*Bs*1(0)	This study
HM663	*trpC2, pheA1, thrC*::P_{xis}-*lacZ* [co-directional] MLS^R, *recA-mGFP*mut2-$spec^R$	This study
HM664	*trpC2, pheA1, thrC*::P_{xis}-*lacZ* [co-directional] MLS^R, *recA-mGFP*mut2-$spec^R$, ICE*Bs*1(0)	This study
HM672	*hisC952, metB5, leuC427,* $SP\beta^{sens}$, xin^{-1}, *thrC::*$P_{spank\ (hy)}$-*metB5* [head-on] MLS^R	This study
HM673	*hisC952, metB5, leuC427,* $SP\beta^{sens}$, xin^{-1}, *thrC::*$P_{spank\ (hy)}$-*metB5* [co-directional] MLS^R	This study
HM674	*hisC952, metB5, leuC427,* $SP\beta^{sens}$, xin^{-1}, *thrC::*$P_{spank\ (hy)}$-*metB5* [head-on] MLS^R, *yqjH::CAT*	This study
HM675	*hisC952, metB5, leuC427,* $SP\beta^{sens}$, xin^{-1}, *thrC::*$P_{spank\ (hy)}$-*metB5* [co-directional] MLS^R, *yqjH::CAT*	This study
HM684	*thrC*::P_{xis}-*lacZ* [co-directional] MLS^R, *recA-mGFP*mut2-$spec^R$, *yqjH::CAT*	This study

HM685	*trpC2, pheA1, thrC*::P_{xis}-*lacZ* [co-directional] *MLS*^{R}, *recA-mGFP*mut2-*spec*^{R}, ICE*Bs*1(0), *yqjH::CAT*	This study
HM706 (BKE23870)	*yqjH::MLS, trpC2*	Bacillus Genetic Stock Center Koo BM *et al.* (In preparation)
HM713 (BKE35160)	*uvrA::MLS, trpC2*	Bacillus Genetic Stock Center Koo BM *et al.* (In preparation)
HM720	*hisC952, metB5, leuC427,* SPβ^{sens}, xin^{-1}, *thrC::*$P_{spank\ (hy)}$-*hisC952* [head-on] *MLS*^{R}, *addAB::KAN*	This study
HM721	*hisC952, metB5, leuC427,* SPβ^{sens}, xin^{-1}, *thrC::*$P_{spank\ (hy)}$-*hisC952* [co-directional] *MLS*^{R}, *addAB::KAN*	This study
HM724	*hisC952, metB5, leuC427,* SPβ^{sens}, xin^{-1}, *amyE::*$P_{spank\ (hy)}$-*leuC427* [head-on] *spec*^{R}, *yqjH::CAT*	This study
HM725	*hisC952, metB5, leuC427,* SPβ^{sens}, xin^{-1}, *amyE::*$P_{spank\ (hy)}$-*leuC427* [co-directional] *spec*^{R}, *yqjH::CAT*	This study
HM726	*hisC952, metB5, leuC427,* SPβ^{sens}, xin^{-1}, *thrC::*$P_{spank\ (hy)}$-*hisC952* [head-on] *MLS*^{R}, *ΔrecA-MLS/CAT*	This study
HM727	*hisC952, metB5, leuC427,* SPβ^{sens}, xin^{-1}, *thrC::*$P_{spank\ (hy)}$-*hisC952* [co-directional] *MLS*^{R}, *ΔrecA-MLS/CAT*	This study
HM730	*hisC952, metB5, leuC427,* SPβ^{sens}, xin^{-1}, *thrC::*$P_{spank\ (hy)}$-*leuC427* [head-on] *MLS*^{R}	This study
HM731	*hisC952, metB5, leuC427,* SPβ^{sens}, xin^{-1}, *thrC::*$P_{spank\ (hy)}$-*leuC427* [co-directional] *MLS*^{R}	This study
HM735	*hisC952, metB5, leuC427,* SPβ^{sens}, xin^{-1}, *amyE::*$P_{spank\ (hy)}$-*hisC952* [head-on] *spec*^{R}, *uvrA::MLS*	This study
HM736	*hisC952, metB5, leuC427,* SPβ^{sens}, xin^{-1}, *amyE::*$P_{spank\ (hy)}$- *hisC952* [co-directional] *spec*^{R}, *uvrA::MLS*	This study

HM737	*hisC952, metB5, leuC427,* SPβ^{sens}, xin^{-1}, *thrC::P$_{spank\ (hy)}$-leuC427* [head-on] *MLS^{R}, yqjH::CAT*	This study
HM738	*hisC952, metB5, leuC427,* SPβ^{sens}, xin^{-1}, *thrC::P$_{spank\ (hy)}$-leuC427* [co-directional] *MLS^{R}, yqjH::CAT*	This study
HM739	*hisC952, metB5, leuC427,* SPβ^{sens}, xin^{-1}, *ΔyqjH*	This study
HM740	*hisC952, metB5, leuC427,* SPβ^{sens}, xin^{-1}, *thrC::P$_{spank\ (hy)}$-hisC952* [head-on] *MLS^{R}, addAB::KAN, yqjH::CAT*	This study
HM741	*hisC952, metB5, leuC427,* SPβ^{sens}, xin^{-1}, *thrC::P$_{spank\ (hy)}$-hisC952* [co-directional] *MLS^{R}, addAB::KAN, yqjH::CAT*	This study
HM742	*hisC952, metB5, leuC427,* SPβ^{sens}, xin^{-1}, *thrC::P$_{spank\ (hy)}$-hisC952* [head-on] *MLS^{R}, ΔyqjH*	This study
HM743	*hisC952, metB5, leuC427,* SPβ^{sens}, xin^{-1}, *thrC::P$_{spank\ (hy)}$-hisC952* [co-directional] *MLS^{R}, ΔyqjH*	This study
HM746	*hisC952, metB5, leuC427,* SPβ^{sens}, xin^{-1}, *thrC::P$_{spank\ (hy)}$-hisC952* [head-on] *MLS^{R}, ΔyqjH, ΔrecA-MLS/CAT*	This study
HM747	*hisC952, metB5, leuC427,* SPβ^{sens}, xin^{-1}, *thrC::P$_{spank\ (hy)}$-hisC952* [co-directional] *MLS^{R}, ΔyqjH, ΔrecA-MLS/CAT*	This study
HM761	*trpC2, pheA1, thrC*::*P$_{xis}$-lacZ* [co-directional] *MLS^{R}, amyE::Pspank (hy)-hisC952 [co-directional] specR*	This study
HM762	*trpC2, pheA1, thrC*::*P$_{xis}$-lacZ* [co-directional] *MLS^{R}, amyE::Pspank (hy)-hisC952 [co-directional] specR,* ICE*Bs1(0)*	This study
HM824	*trpC2, pheA1, thrC*::*P$_{xis}$-lacZ* ICE*Bs1*(0), *ΔrecA-MLS/CAT*	This study
HM874	*hisC952, metB5, leuC427,* SPβ^{sens}, xin^{-1}, *amyE::P$_{spank\ (hy)}$-hisC952* [head-on] *spec^{R}, mfd*::Cm^{R}, *yqjH::MLS*	This study
HM875	*hisC952, metB5, leuC427,* SPβ^{sens}, xin^{-1}, *amyE::P$_{spank\ (hy)}$- hisC952* [co-directional] *spec^{R}, mfd*::Cm^{R}, *yqjH::MLS*	This study

HM1102	*hisC952, metB5, leuC427,* SPβ^{sens}, xin^{-1}, *amyE::P$_{spank\ (hy)}$-hisC952* [head-on] *spec^{R}, uvrA::MLS*	This study
HM1103	*hisC952, metB5, leuC427,* SPβ^{sens}, xin^{-1}, *amyE::P$_{spank\ (hy)}$- hisC952* [co-directional] *spec^{R}, uvrA::MLS*	This study
HM1177	*hisC952, metB5, leuC427,* SPβ^{sens}, xin^{-1}, *amyE::P$_{spank\ (hy)}$-hisC952* [head-on] *spec^{R}, uvrA::MLS*	This study
HM1178	*hisC952, metB5, leuC427,* SPβ^{sens}, xin^{-1}, *amyE::P$_{spank\ (hy)}$- hisC952* [co-directional] *spec^{R}, uvrA::MLS*	This study
HM1279 (BKE35710)	*uvrB::MLS, trpC2*	Bacillus Genetic Stock Center Koo BM *et al.* (In preparation)
HM1280 (BKE28490)	*uvrC::MLS, trpC2*	Bacillus Genetic Stock Center Koo BM *et al.* (In preparation)
HM1281	*hisC952, metB5, leuC427,* SPβ^{sens}, xin^{-1}, *amyE::P$_{spank\ (hy)}$-hisC952* [head-on] *spec^{R}, uvrB::MLS*	This study
HM1282	*hisC952, metB5, leuC427,* SPβ^{sens}, xin^{-1}, *amyE::P$_{spank\ (hy)}$- hisC952* [co-directional] *spec^{R}, uvrB::MLS*	This study
HM1283	*hisC952, metB5, leuC427,* SPβ^{sens}, xin^{-1}, *amyE::P$_{spank\ (hy)}$-hisC952* [head-on] *spec^{R}, uvrC::MLS*	This study
HM1284	*hisC952, metB5, leuC427,* SPβ^{sens}, xin^{-1}, *amyE::P$_{spank\ (hy)}$- hisC952* [co-directional] *spec^{R}, uvrC::MLS*	This study

Table S3. Plasmids used or generated in this study.

Plasmid	Relevant features	Integration locus	Reference
pDR111	*amp*^{R}, *amyE::P*$_{spank(hy)}$, *lacI*, *spec*^{R}	*amyE*	Guérout-Fleury, Gene. 1996
pCAL838	*amp*^{R}, *thrC::P*$_{spank(hy)}$, *lacI*, *spec*^{R}	*thrC*	Guérout-Fleury, Gene. 1996
pHM85	*P*$_{spank(hy)}$-*leuC427* [head-on] *spec*^{R}	*amyE*	This study
pHM89	*P*$_{spank(hy)}$-*leuC427* [co-directional] *spec*^{R}	*amyE*	This study
pHM88	*P*$_{spank(hy)}$-*hisC952* [head-on] *spec*^{R}	*amyE*	Paul, Nature, 2013
pHM91	*P*$_{spank(hy)}$-*hisC952* [co-directional] *spec*^{R}	*amyE*	Paul, Nature, 2013
pHM95	*P*$_{spank(hy)}$-*metB5* [head-on] *spec*^{R}	*amyE*	This study
pHM96	*P*$_{spank(hy)}$-*metB5* [co-directional] *spec*^{R}	*amyE*	This study
pHM59	*P*$_{spank(hy)}$-*hisC952* [head-on] *MLS*^{R}	*thrC*	This study
pHM60	*P*$_{spank(hy)}$-*hisC952* [co-directional] *MLS*^{R}	*thrC*	This study
pHM107	*P*$_{xis}$-*lacZ* [co-directional] *MLS*^{R}	*thrC*	This study
pHM111	*P*$_{spank(hy)}$-*metB5* [head-on] *MLS*^{R}	*thrC*	This study
pHM112	*P*$_{spank(hy)}$-*metB5* [co-directional] *MLS*^{R}	*thrC*	This study
pHM115	*P*$_{spank(hy)}$-*leuC427* [head-on] *MLS*^{R}	*thrC*	This study
pHM116	*P*$_{spank(hy)}$-*leuC427* [co-directional] *MLS*^{R}	*thrC*	This study
pDR244	*cre*, *spec*^{R}, *amp*^{R}, pE194-ts	N/A	Bacillus Genetic Stock Center
pMMB124	*kan*^{R}	*cgeD*	Guérout-Fleury, Gene. 1996
pKG1	*P*$_{xis}$-*lacZ* [head-on] *MLS*^{R}	*thrC*	Merrikh, *Nature*, 2011

Table S4. Oligonucleotides used in this study

#	Sequence
HM112	CGCGTCAACAGGTAACACTTCC
HM115	GGATCTTTCAGTCCGTTTCC
HM188	GGCTTTCGCTACCTGGAGAG
HM189	GACGAAGCCGCCCTGTAAAC
HM192	CCGTCTGACCCGATCTTTTA
HM193	GTCATGCTGAATGTCGTGCT
HM205	TCCAAACTGGACACATGGAA
HM207	AAAGAGGCGTACTGCCTGAA
HM265	GCTCAGTTTTTGAGCGATATAGG
HM266	CGCACAGATGCGTAAGGAGAAACAAATCTCCTTTTCGGTCA
HM267	TAATATGAGATAATGCCGACTGTACATCGCTTGAAAAAAAGGG
HM268	TACACGCTCTTCCTTCATAGCTGAGATAAA
HM328	TCAAAATGTGCTCCAGGTGA
HM329	CAAGCTTGAGTATCTATAGTGTCTATCCCTATCCGGTGCCATA
HM330	CGCAACTGTCCATACTCTGATGGTGAAAGCATTTGCGGATTT
HM331	CTTCAAAAACCGGCCTGATA
HM382	AAAAGTCGACAAGGAGGTATACATATGATGCCTCGAACAATCATCG
HM386	AAAAGTCGACAAGGAGGTATACATTTGCGTATCAAAGAACATTTAAAAC
HM388	AAAGAATTCTTACACAACTGTTTTTTCC
HM389	AAAGCATGCTGGCAAGAACGTTGCTCGAGG
HM390	AAAGAATTCTTAGTCCCATTCATAAGG
HM391	AAAAGCTAGCTGGCAAGAACGTTGCTCGAGG
HM392	AAAGAATTCTAACTCACATTAATTGCGTTGC
HM393	AAAGGATCCTGGCAAGAACGTTGCTCGAGG
HM394	AAAAGCTAGCTCCTTATGAATGGGACTTACACAACTGTTTTTTCCTG
HM395	AAAGAATTCTCCTTATGAATGGGACTTACAC
HM396	AAAGCATGCTCCTTATGAATGGGACTTATAAAATTTCAGCTAAAATGG
HM489	AGTCGGATACGGAATTGCTG
HM490	CCCAGACGGCTGGTATTAAA
HM495	ACGATCGGAACAAAAGAGCA
HM496	TTTCCACCGAATTAGCTTGC
HM657	TGAGCGGATAACAATTAAAGGAGGTATACATttgCCTATTAATATACCAACACACC
HM658	AGCTTGCATGCGGTTAGTCCCATTCATAAGG
HM770	TCTCCAGCTGTGATAAACGGTA

HM771	AAAACGGCATTGATTTGTCA
HM805	AAAAGCGGCCGCATCGAATTCGATAACCCTAAAGTTATG
HM806	AAAAGCATGC TAATAACCGGGCAGGCCAT
HM807	AAAAGCGGCCGCTTATTTTTGACACCAGACCAA
HM808	AAAAGCATGCAAGCTTCCGATATTAAGTTTCTCTG
HM958	AGC TTT GTT ATT GCT GGC AAT GTC G
HM959	TAC ATA CTT TTC CCG GTC CGA TGC
HM960	CGA AGG ACA TAC ATT TCC CTG CAG C
HM961	GCT TAC GAA GGA ACG ACC AGA GC
HM793 a-h	CAAGCAGAAGACGGCATACGAGAiiiiiiiiTCGTAACCAGATGAAGCACTCTTTCCACT ATCCCTACAGTGT
HM794	ACACTCTTTCCCTACACGACGCTCTTCCGATCT
HM795	ACACTGTAGGGATAGTGGAAAGAGTGCTTCATCTGGTTACGA
HM796	TGC GTT TCC TGA CCG GAC GAT ATA GCC TTT TTC CAG C
HM792	AATGATACGGCGACCACCGAGATCTACA ACACTCTTTCCCTACACGACGCTCTTCCGATCT NNNN*TTAAACGTCCTGCTGATGAAC*

Detailed plasmid construction

Plasmids were constructed using standard molecular biological techniques. All plasmids were propagated in *E. coli* DH5α under ampicillin selection. Plasmids were isolated using the 5-Prime Plasmid Mini kit. PCR reactions used Phusion Flash DNA polymerase (Thermo) or the Extend Long-Template PCR system (Roche). Linear DNA fragments were isolated using the 5-Prime Agarose Gel Extract kit. DNA was digested and ligated using Fast Digest Restriction Enzymes and Rapid Ligase with the appropriate buffers (Fermentas).

pHM88 and pHM91 were constructed as described previously. pHM85 was constructed by amplifying the *leuC427* allele from HM380 genomic DNA using the primers HM382 and HM394. The PCR fragment was digested with SalI and NheI and ligated into pDR111, which had been cut with the same enzymes. pHM86 was constructed by amplifying the *leuC427* allele as well as $P_{spank(hy)}$ from pHM85 using primers HM388 and HM389. The fragment was digested with EcoRI and SphI and subsequently ligated into pDR111, which had been digested with the same enzymes. pHM59 and pHM60 were constructed by digesting pHM88 and pHM91 with EcoRI and BamHI and ligating the fragments into pCAL838. pHM115 and pHM116 were built using a similar strategy, except the enzymes used were EcoRI and NheI for pHM115 and EcoRI and SphI for pHM116.

pHM95 was constructed by amplifying the *metB5* allele from HM380 genomic DNA using primers HM657 and HM658. The PCR product was introduced into pDR111 that had been linearized by HindIII/NheI digestion via isothermal assembl. pHM96 was

constructed by amplifying the *metB5* allele as well as $P_{spank(hy)}$ from pHM95 using primers HM390 and HM391. The PCR product was digested with EcoRI and NheI and ligated into pDR111. pHM107 was generated based upon plasmid pKG1. The pKG1 plasmid backbone (excluding P_{xis}-*lacZ*) was amplified using primers HM805 and HM806. The P_{xis}-*lacZ* fragment was amplified using primers HM807 and HM808. The resulting fragments were digested with NotI and SphI and ligated together with the insert in the opposite orientation.

Detailed strain construction

HM391 was generated by transformation of a linear PCR product into HM1. The primers used to construct the *yqjH::CAT* deletion product were HM265, HM266, HM267, and HM268. pGEM-*cat* served as the template for the chloramphenicol resistance marker. HM400 was generated by transforming HM380 with genomic DNA from HM391. HM 449, and 450; HM672, and 673; HM730 and 731 were constructed by introducing pHM59 and pHM60; pHM111 and pHM112; and pHM115 and pHM116 into HM380 and selecting MLS^R. Integration at thrC was confirmed both by threonine auxotrophy and PCR across the *thrC* locus using primers HM112 and HM115.

HM417/HM418 and HM632 and HM633 were generated by transforming pHM85/89 and pHM95/96 into HM380 and selecting for spectinomycin resistance. Integration at amyE was confirmed via starch-plate assay as well as PCR across the *amyE* locus using primers HM205 and HM207. HM421, HM422, HM611, HM612, HM634, HM635, HM674, HM675, HM 724 and HM725, and HM737 and 738 were generated by transforming the above-described strains with genomic DNA from HM400 and selecting for chloramphenicol resistance. Replacement of the *yqjH* gene with the chloramphenicol resistance cassette was confirmed by PCR using primers HM265 and HM266.

HM594, HM595, HM596 and HM597 were generated by transforming HM449, HM450, HM611 and HM612 with genomic DNA from HM313 and selecting for spectinomycin resistance. Presence of the RecA-GFP tag was confirmed by microscopy.
HM210 and HM211 were constructed as described previously (Merrikh). HM352 and HM630 were generated by transformation of HM210 and HM211 with genomic DNA isolated from HM313. HM629 and HM 621 were generated by transformation of HM352 and HM630 with genomic DNA from HM391. HM639 and HM640 were generated by introducing pHM107 into HM1 and HM253. These strains were transformed with genomic DNA from HM313 to generate strains HM663 and HM664. Transformation of HM663 and HM664 with genomic DNA from HM391 yielded strains HM684 and HM685.
HM415 was constructed in the same manner as HM391 except the primers used were: HM329, HM330, and HM331. pMMB124 served as the template for the kanamycin resistance cassette HM720 and HM721 were constructed by transforming genomic DNA from HM415 into HM449 and HM450, and selecting for kanamycin resistance. HM740 and 741 were constructed by transforming genomic DNA from HM400 into HM 720 and 721 and selecting for chloramphenicol resistance.

HM735 was constructed by transforming genomic DNA from BKE23870 into HM380 and selecting for MLS^R. HM7395 was transformed with pDR244, which encodes a functional *cre* gene, and selected for spectinomycin resistance in order to generate

strain HM740: a markerless deletion of *yqjH*. pDR244 was evicted from HM739 by 24 hours growth at 42°C. Loss of the MLS^R marker was confirmed by sensitivity and PCR across the *yqjH* locus. Loss of the plasmid was confirmed by spectinomycin sensitivity. HM739 was transformed with pHM59 and pHM60 to generate HM742 and HM743. HM742 and HM743 were transformed with genomic DNA from HM209 and selecting for chloramphenicol resistance to generate HM746 and 746.

Detailed media compositions

The concentrations for each antibiotic used were: spectinomycin (50 μg/ml), kanamycin (50 μg/ml), chloramphenicol (50 μg/ml), or lincomycin and erythromycin at 25 μg/ml each. *E. coli* was grown in LB supplemented with ampicillin at 100 μg/ml.
To determine viabilities for fluctuation analyses, *B. subtilis* cells were plated on solid agar plates containing Spizizen's Minimal Medium (0.2 mg/ml ammonium sulphate, 1.4 mg/ml monobasic potassium phosphate, 0.6 mg/ml dibasic potassium phosphate, 0.1 mg/ml sodium citrate dihydrate, 0.02 mg/ml magnesium sulphate heptahydrate, 100 μg/ml glutamic acid, 5 μg/ml glucose), supplemented with isoleucine, methionine, leucine and histidine at 50 μg/ml. To select for reversion to prototrophy in fluctuation analyses, cells were plated on solid agar plates containing essentially the above medium, lacking the amino acid corresponding to the reporter gene to be tested.

Survival assays

Exponentially growing pre-cultures (OD 0.3-0.6) were set back to OD 0.05 in LB, and grown to exponential phase again (OD 0.3-0.6). Cells were serially diluted $1:10^{-5}$ and 5 μl of each dilution were spotted onto LB agar plates either supplemented or not with 4-Nitro-Quinolone Oxide with 2 technical replicates per isolate. To determine UV sensitivity cells were spotted onto LB agar plates and exposed to UV using a Mineralight XX 15V UV light source (UVP). Surviving colonies were enumerated after overnight incubation at 30°C.

Growth curves

Exponentially growing pre-cultures were diluted to OD=0.005 into minimal medium lacking histidine and supplemented with 1mM IPTG (to induce transcription of the particular *hisC* allele). Cultures were aliquoted into the wells of a clear-bottomed 96-well plate. ODs were measured at seven-minute intervals using a Biotek Synergy H1 plate reader, using a kinetic program with continuous shaking at 37°C.

Supplemental References

1) Yasbin, R. E., R. Miehl-Lester, and P. E. Love. 1987. Mutagenesis in *Bacillus subtilis*, p. 73-84. *In*M. Alacevic, D. Hranueli, and Z. Tomen (ed.), *Genetics of industrial microorganisms*. GIM-86, Split, Yugoslavia.
2) Guérout-Fleury AM, Frandsen N, Stragier P. Plasmids for ectopic integration in Bacillus subtilis. *Gene*. 1996;180(1-2):57–61.
3) Miller, J. 1972. Experiments in Molecular Genetics, p. 352-355. Cold Spring Harbor Laboratory, NY.